

---

# Experimental Investigation of the Hygrothermal Performance of Insulation Materials

Kurt K. Hansen, Ph.D.

Carsten Rode, Ph.D.

Ernst J. de Place Hansen, Ph.D.

Tim Padfield, Ph.D.

Finn Kristiansen

## ABSTRACT

*Apparatus, methods, and test results from an experimental investigation of (1) the effect of moisture on the thermal conductivity of insulation materials, (2) the properties for moisture performance of the materials, including water sorption, water vapor transmission, and capillary water uptake, and (3) humidity buffering of the indoor climate by an absorbent wall are presented.*

*The materials are cellulose fiber, flax, sheep's wool, perlite, rock fiber, and glass fiber. Rock fiber and glass fiber are materials currently used in Denmark.*

*The test results can be summarized as follows: The thermal conductivities of the materials are not much affected by RH until dew point is reached at the cold side of the test specimen. Some of the properties for moisture performance of the materials are very dependent on the type of material. The results from the sorption measurements confirm previously published data for the pure materials but show that added salts increase the water absorption at a high RH. The capillary water uptake tests show that perlite treated with silicon resin, sheep's wool, flax, rock fiber, and glass fiber have a small water absorption capacity and a small short-term water absorption coefficient. The water vapor permeability, measured at a steady state, is similar for the tested materials. Humidity buffering of the indoor climate by an absorbent wall has no practical influence on the indoor climate of a house if the house is ventilated as recommended.*

*The test results are discussed and interpreted due to use of the materials in practice.*

---

## INTRODUCTION

In the light of the growing interest in “green” or “environmentally friendly” building systems, the Danish government supports a research program on environmentally friendly insulation materials (i.e., materials that are “alternative” to the materials currently found on the Danish market).

We present apparatus, methods, and test results from an experimental investigation of (1) the effect of moisture on the thermal conductivity of the insulation materials, (2) the properties for moisture performance of the materials, including water sorption, water vapor transmission, and capillary water uptake, and (3) humidity buffering of the indoor climate by an absorbent wall.

The materials are the organic fibers, cellulose fiber, flax, and sheep's wool and the inorganic perlite, rock fiber, and

glass fiber. Rock fiber and glass fiber are currently the most used insulating materials in Denmark.

The materials are identified and described in Table 1. The whole investigations are reported also by Hansen (1999).

## THERMAL CONDUCTIVITY AT DIFFERENT HUMIDITIES

The thermal conductivity was determined with a guarded hot plate apparatus modified to maintain defined humidity conditions over the specimen. The principle of the modified hot plate apparatus is shown in Figure 1. This apparatus was developed from a the prototype by Lund Madsen (1969).

Previously, Tye and Spinney (1979) studied the effect of moderate moisture on thermal performance in wall constructions with cellulose insulation. They found a decrease of the

---

**Kurt Kielsgaard Hansen** is an associate professor and **Ernst Jan de Place Hansen** is an assistant research professor, Department of Structural Engineering and Materials, Technical University of Denmark, Lyngby, Denmark. **Tim Padfield** is a scientist, Conservation Department, The National Museum of Denmark, Lyngby, Denmark. **Carsten Rode** is an associate professor and **Finn Kristiansen** is an assistant research professor, Department of Buildings and Energy, Technical University of Denmark.

**TABLE 1**  
**Identification and Description of Materials**

Name	Description	Density [kg/m <sup>3</sup> ]
Cellulose-1	Recycled paper fibers with 18% of borate salts (L)	40 or 65
Cellulose-2	Recycled paper fibers with 5% of borate salts (L)	40
Cellulose-3	Recycled paper fibers with 6% of borate salts and 9% of aluminum hydroxide (L)	40
Cellulose-4	Recycled paper fibers without salts (L)	40
Sheep's wool	Sheep's wool with 2% to 4% of boron salts (C)	25
Flax	Flax with 8% of ammonium phosphate/sulphate (C)	30
Perlite SR	Expanded volcanic glass with 0.2% of silicon resin (L)	85±20
Perlite	Expanded volcanic glass, without water repellent (L)	85±15
Rock fiber	Rock fiber with 0.5% silicon oil (C)	30 to 32
Glass fiber	Glass fiber with 1% silicon oil (C)	16

Notes: Additive concentrations are in weight percent. Perlite has grain size of 0.5 to 0.6 mm. Cellulose-1 is tested in two different densities. Flax contains 18% of polyester fibers as support. (L) is loose fill material, while (C) is coherent material.

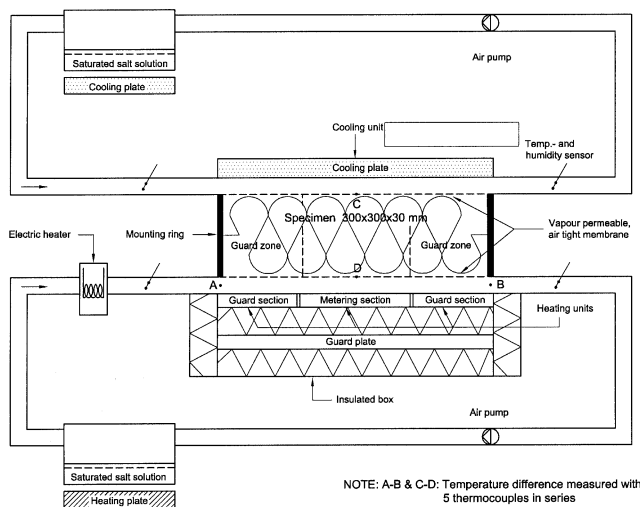


**Figure 1** Outline of the modified guarded hot plate apparatus. Conditioned air is circulating in channels immediately below and above the specimen.

thermal resistance by 15% when the moisture content increased by 10% and judged this not to be dramatic. In contrast to this previous study, the present investigation is focused on thermal conductivity measurements of the insulation material alone, and measurements are carried out for several different insulation materials.

### Description of the Apparatus

The apparatus consists of a hot and a cold plate. The power supplied to the hot plate is determined by measuring the

electric current and the voltage. The humidity level in air gaps on each side of the test specimen is adjusted by means of air circulating through boxes with temperature-controlled saturated salt solutions. In this way, it is possible to apply controlled levels and gradients of humidity over the specimen (see Figure 2). In the 160-by-160-mm metering section, power is supplied by the heating unit under the test specimen. The cold side is kept at about 14°C and the hot side at about 28 °C. The temperature difference, C-D, between the two sides of the test specimen is measured with a thermopile with five thermocouples placed within the metering section. The surface of the test specimen is 300 by 300 mm and it is 30 mm thick. The heat flow above the metering section is almost perfectly one-dimensional according to a three-dimensional calculation.

Two measures are taken to ensure one-dimensional heat flow through the test material:

1. A guard section and a guard plate prevent the heat from the metering section from being lost to the sides or through the bottom of the insulated box. The guard section and the guard plate have the same temperature as the hot plate of the metering section.
2. The difference between the air inlet and outlet temperatures (A-B) over the hot plate is controlled and kept at 0 K by means of a small heating element placed immediately before the air inlet. By this construction it is ensured that the air does not remove power from the area around the hot plate.

The apparatus was checked without air circulation to determine the thermal conductivity of XPS insulation: the results were within 3% of expectation. With air circulation, the results were within 11%.

The test specimen is sandwiched between layers of spun-bonded polyolefin to minimize the flow of air through it. The thermopile C-D is mounted on the inside of the membranes. At

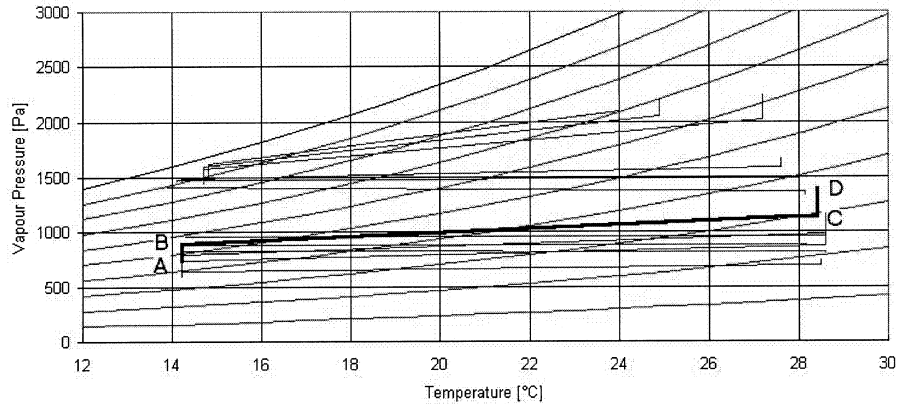


**Figure 2** Vapor pressure diagram showing the test conditions in the air channels and at the two surfaces of the specimen. The curved lines show RH in steps of 10%. Each of the angled lines indicates one of the 13 different test conditions over the specimen. The thick, angled line is an example of one such condition.

- Point A is the condition in the airstream on the cold side (14.2°C, 743 Pa)
- Point B is the condition in the interface between polyolefin membrane and specimen on the cold side (14.2°C, 917 Pa).
- Point C is the condition in the interface between polyolefin membrane and specimen on the warm side (28.4°C, 1214 Pa).
- Point D is the condition in the airstream on the warm side (28.2°C, 1388 Pa).

each inlet and outlet of the air gaps over and below the specimen—four places in all—the temperature and the humidity (% RH) of the air are measured.

The circulation of air over and under the specimens caused small air pressure differences over the specimens that are measured to be up to 20 Pa. With air permeability data for spun-bonded polyolefin, the convective heat flow through the otherwise permeable specimens could be estimated. It was found to be around 7% of the magnitude of the heat flow by conduction through the specimens. With the specimens and temperature differences used in the experiments, it can be assumed that natural convection does not occur internally in the specimens.

### Measurements and Results

The thermal conductivity of the material is first measured using airflow but without humidity conditioning of the air. The subsequent measurements are made with airflow under different conditions of increasing humidity. First, the measurements are made with degrees of humidity typical of the room air (about 30% to 50% RH). Subsequently, the humidity in the air gaps is gradually increased. At the end of the measurement, condensation arises in the material.

For each material, the thermal conductivity is determined in up to 13 steps with different levels of relative humidity (see Figure 2). The measurement period for each step lasted until

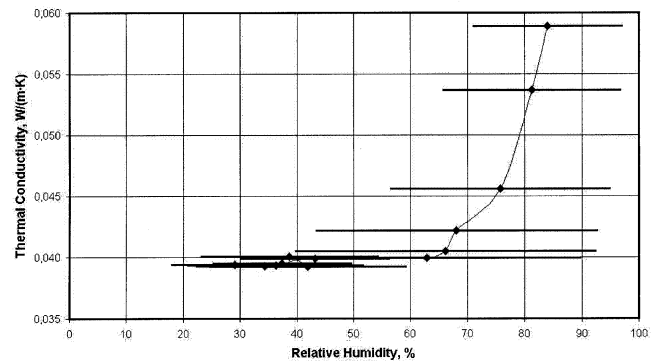


**Figure 3** Thermal conductivity for cellulose-1 as a function of relative humidity over the surfaces of the specimen. The horizontal lines link the RH at each side of the specimen. The curved line follows the mean value.

the heat flow had become steady—typically two to five days. When the heat and vapor flow becomes steady, and there is no condensation in the specimen, the measurement is not disturbed by latent heat flows. However, during the last three to six steps in each sequence, condensation has most likely formed on the cold side of the insulation, as also verified at the end of the experiment when the setup was taken apart. The heat flow never settled at a definite value during these steps. The results from these last steps with condensation are mean-

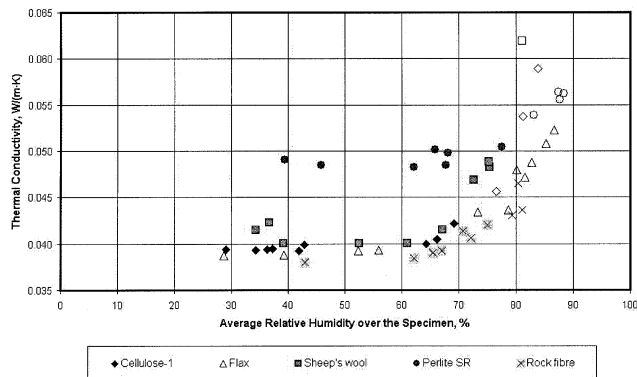


**Figure 4** Thermal conductivity for the tested materials recorded as a function of the average relative humidity on the two sides of the test specimen. Measurements where condensation takes place are shown with open symbols.

ingless and, therefore, shown with separate signatures (open symbols) in the presentation of results (Figure 4).

Figure 3 shows the measured thermal conductivity as a function of the relative humidity on the two sides of the specimen. The thermal conductivity is rather constant at most humidity levels and then increases significantly when the relative humidity is in the range from 90% to 100% RH on the cold side. For the high humidities, the thermal conductivity increases by up to 50%—or possibly more if interstitial condensation is allowed to continue. The values of relative humidity given in the figure have been determined for the interface between insulation and airtight membrane using steady-state diffusion theory, measured vapor diffusion resistance for spun-bonded polyolefin, and measured vapor permeability of the material. The vapor diffusion resistance used for spun-bonded polyolefin in this calculation was an interpolated result between dry- and wet-cup values to approximate the humidity conditions of the membrane on the cold and warm sides of the insulation in each of these experiments.

Due to various inaccuracies of the modified apparatus so the humidity influences can be controlled, the results cannot be seen as definitive measurements of thermal conductivity of the tested materials. The results show the relative influence on thermal conductivity of exposing the specimen to humidity and also humidity gradients at various levels.

For all the materials, the thermal conductivity is rather constant at most humidity levels and then increases significantly when the mean relative humidity is above 70% RH (Figure 4). However, the extent at which this increase is caused by an accumulation of humidity as condensation in the parts of the insulation that are close to the cold side is somewhat uncertain. Thus, the measured greater thermal conductivities have no practical importance in structures without

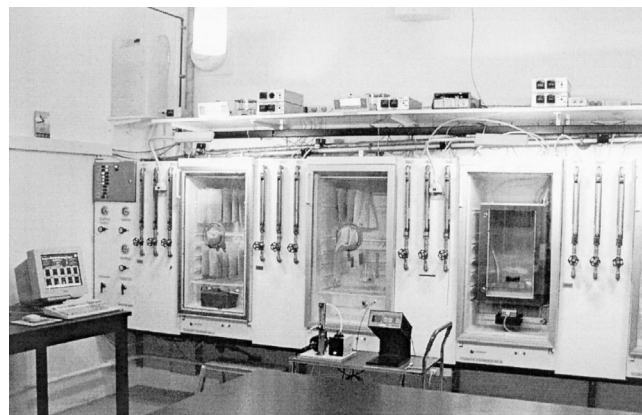


**Figure 5** Climate chamber setup for determination of sorption isotherms. The specimen hanging in polyester bags can be weighed without removing them from the chamber.

condensation. Disregarding these condensation situations, the maximum increase in the thermal conductivity is 5% to 10%, owing to the hygroscopic uptake of humidity from the ambient air. This corresponds well with previous findings by Tye and Spinney (1979) for cellulose insulation.

## SORPTION ISOTHERMS

The sorption isotherms are measured at  $20.0^{\circ}\text{C} \pm 0.5^{\circ}\text{C}$  in a test chamber as described in prEN ISO 12571 (CEN 1998). The specimens are weighed without removing them from the test chamber (Figure 5). This is essential since the fibrous material reacts very fast with the environment. The specimens are placed in bags made of polyester net with a mesh size of  $73\ \mu\text{m}$ . The materials, as delivered, were exposed in bags in the test chamber at 3% RH until equilibrium. Thereafter, the absorption isotherms were measured up to 96% RH, and then the desorption isotherms were determined. Finally the specimens were dried at less than 1% RH over magnesium perchlorate desiccant until equilibrium.

## Measurements and Results

Figure 6 shows the absorption and desorption isotherms based on the mass after final drying by means of magnesium perchlorate. The curves for perlite SR do not differ significantly from untreated perlite.

The sorption curves of these fibers have been reported many times in the literature. The interest of the curves presented here is in how the added salts modify the expected behavior. Two materials are selected for detailed discussion. Their isotherms are shown in Figure 7. The expected isotherm for the cellulose material is shown in Figure 7a. This same raw material, with added borax and boric acid, gives the pattern shown in Figure 7b. The starting material gains weight to 96%

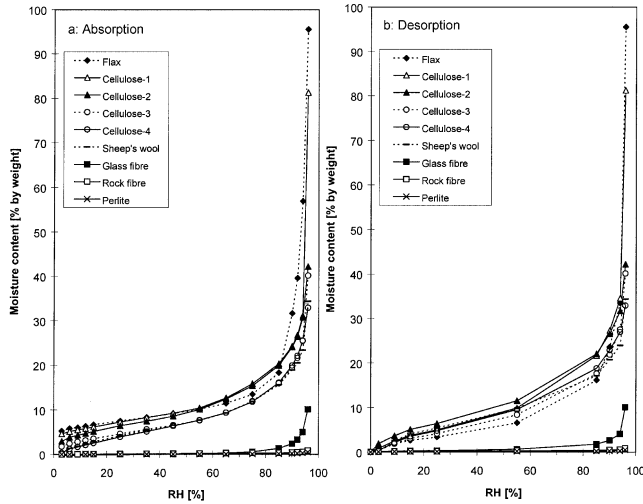


**Figure 6** Absorption (a) and desorption (b). The materials are listed with the most hygroscopic material first. The origin for both sets of curves is based on the weight after a final drying at <1% RH over magnesium perchlorate.

RH. At this high RH, the moisture content is greater than that of the pure material, indicating that the salts are enhancing the water absorption and presumably are themselves dissolving and being absorbed into the fibers. Then, on the return to dryness, the curve remains unexpectedly close to the absorption curve and in the end crosses over to end at 3% RH below the starting point. We attribute this to a permanent change in the sodium borate, perhaps to a state where it is bound as ions within the fiber and is not in the hydrated crystalline form in which it started. The third graph (Figure 7c) is for flax with an ammonium phosphate/sulphate fire retarder. It shows more extreme behavior, with the desorption curve always below the absorption curve. Notice also the very high absorption at high RH, surely due to water absorption by the salt. Separate measurements on the salts are shown in Table 2.

This confirms the assumption that sodium borate is bound as ions within the fibers. The phenomenon of enhanced water absorption by organic fibers with added inorganic salts, even at an RH below the deliquescence point of the pure salt, is described by Padfield and Erhardt (1987) for the silk-sodium chloride system.

The sharp jump in the sorption curves from 0% to 3% in Figure 6 is an artifact of the calculation process. There is an irreversible change in the status of the salt as the material passes through its first experience of a high RH. If this is calculated out, one gets quite close to the expected isotherm for the pure material for the region 0% to 80% RH, with an enhanced absorption at high RH due to the added salt.

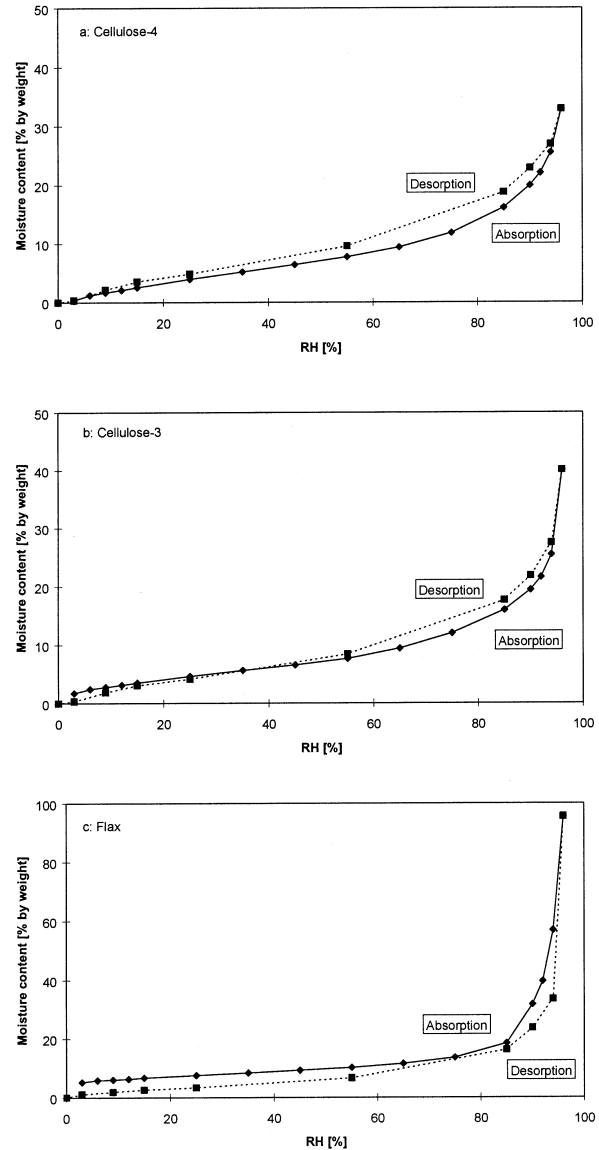


**Figure 7** Sorption isotherms. a: cellulose fiber (cellulose-4) without salts; b: cellulose fiber (cellulose-3) with salts; c: flax with salts. Moisture contents are based on the weight after drying over magnesium perchlorate desiccant.

**TABLE 2**  
Absorption in Weight Percent Measured on Pure Salts from the Materials at 21°C

Salt	44% RH	86% RH	97% RH	100% RH
Boric acid	0	0	0	70
Borax	0	1.3	1.7	20
Aluminum hydroxide	0	0	0.3	0.7
Ammonium phosphate/sulphate	0	128	198	709

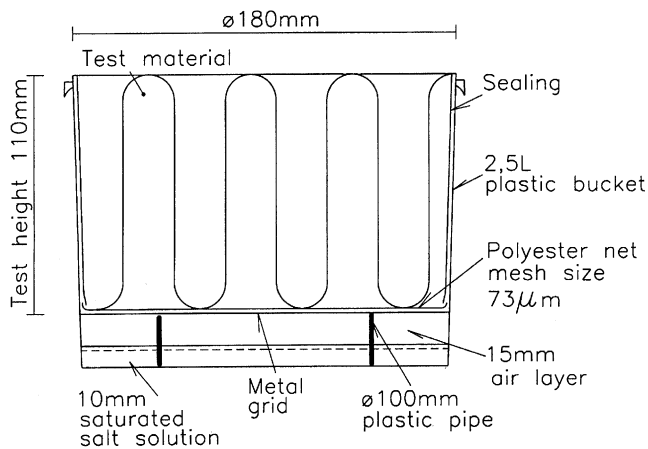


**Figure 8** Cup used for the permeability measurements.

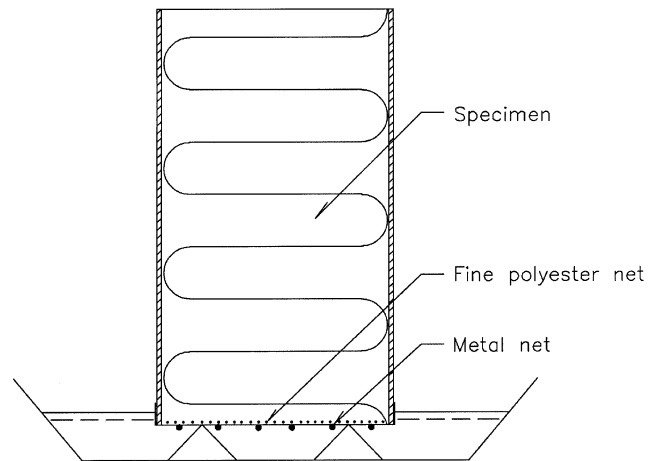
## WATER VAPOR PERMEABILITY

The cup method is used, as described by Hansen (1989). The test specimen forms the lid of a cup above a desiccant or a saturated salt solution to control the RH. The cup is exposed to an airstream of another RH. The loss or gain of weight is recorded. The cup design is shown in Figure 8. The chamber temperature is  $23.0^{\circ}\text{C} \pm 0.3^{\circ}\text{C}$ , and the RH is  $50\% \pm 2\%$ . The climate inside the cup is 94% RH (saturated potassium nitrate solution) or less than 1% RH (magnesium perchlorate desiccant). The permeability is determined by weighing the cup periodically and measuring the rate of change when a steady rate is reached. The equations used for calculating water vapor transmission are described in prEN ISO 12572 (CEN 1998) and by Hansen and Lund (1990), who give formulas for corrections for the surface resistances at the specimen surfaces and the diffusion resistance in the air layer inside the cup. The surface resistances are calculated based on Lewis' law, while the resistance in the still air is calculated as air layer thickness divided by water vapor permeability of still air. Lackey et al. (1997) also make these corrections for highly permeable materials.

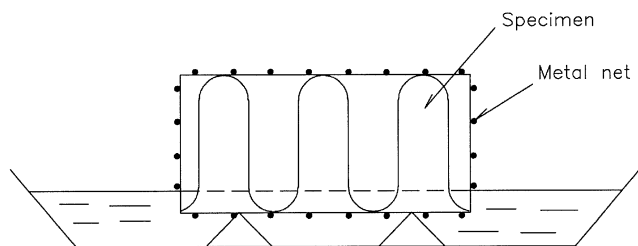
### Measurements and Results

Table 3 shows the water vapor diffusion resistance ( $Z$ ) and the water vapor permeability ( $\delta$ ) from the cup measurements at  $23^{\circ}\text{C}$  with 50% RH in the chamber and 94% RH in the cup. The diffusion resistance and permeability are first calculated according to the standard prEN ISO 12572 (CEN 1998). The second column gives corrected values according to Hansen and Lund (1990).

The measured permeabilities (Table 3) indicate that all the materials are very permeable to water vapor. Some of the corrected permeability values are in the order of or above the value for still air. For these very permeable materials, the corrections are large and maybe on the order of what can be allowed. However, the corrections are verified by separate



**Figure 9** Setup for measurement of water absorption capacity for loose fill materials.



**Figure 10** Setup for measurement of water absorption capacity for coherent materials.

measurements on empty cups. Lackey et al. (1997) show the measured permeability for medium density glass fiber insulation board (dry density  $54 \text{ kg/m}^3$ ) in the vicinity of 100% RH approaches that of still air.

Perlite SR and cellulose-1 at  $65 \text{ kg/m}^3$  are the least permeable of the tested products, while cellulose-1 at  $40 \text{ kg/m}^3$  and cellulose-3 at  $40 \text{ kg/m}^3$  are the most open—about twice as much as the least permeable. In general, the permeability of the tested materials, with 1% RH in the cup (not shown in Table 3), is within 10% to 15% of the permeability with 94% RH in the cup.

## CAPILLARY WATER UPTAKE

In these tests, the material forms a column whose lower end dips into water. The water absorption capacity, the mean water content, and the short-term liquid water absorption coefficient are determined. Figure 9 shows the setup for loose fill materials, and Figure 10 shows the setup for coherent materials. The setup in Figure 9 consists of a plexiglass tube containing the test specimen with a steel net at the bottom on which a fine polyester net is placed. There is no lid on the tube, which means that evaporation is not prevented. The setup in Figure 10 consists of a "cage" of steel net, with variable height containing the test specimen. The climate in

**TABLE 3**  
**Water Vapor Diffusion Resistance (Z) and Permeability ( $\delta$ ) under an**  
**RH Gradient of 50% to 94% at 23°C**

Material	Density [kg/m <sup>3</sup> ]	Thickness before test [mm]	Settling during test [% of init. thickness]	Z [10 <sup>9</sup> (Pa s m <sup>2</sup> ) / kg]		$\delta$ [10 <sup>-12</sup> kg / (Pa m s)]	
				Values according to standard <sup>1</sup>	Adjusted values <sup>2</sup>	Values according to standard <sup>1</sup>	Adjusted values <sup>2</sup>
Cellulose-1	40	110	< 5	0.66±0.04	0.54±0.04	170±10	203±15
Cellulose-1	65	115	0	1.15±0.02	1.03±0.02	93±6	110±0
Cellulose-3	40	110	5	0.62±0.09	0.51±0.09	177±29	223±40
Cellulose-3	40	50	< 10	0.44±0.05	0.33±0.05	113±15	153±25
Cellulose-4	40	110	< 5	0.78±0.13	0.66±0.13	147±25	173±31
Sheep's wool	25	100	0	0.72±0.14	0.60±0.14	160±35	190±52
Flax	30	30	0	0.28±0.11	0.16±0.12	120±46	150±57
Perlite SR	85	110	0	1.14±0.15	1.02±0.15	90±10	103±15
Rock fiber	32	50	0	0.40±0.05	0.28±0.06	127±15	183±31
Glass fiber	16	50	0	0.38±0.09	0.27±0.09	137±38	155±7

Notes:  
<sup>1</sup>: prEN ISO 12572 (1998). <sup>2</sup>: Adjusted for air layer thickness and surface diffusion resistances.  
 Values for diffusion resistance Z and permeability  $\delta$  are mean values  $\pm$  spread (three specimens).  
 Air layer inside cup is 15 mm, wind speed above cups is about 3 m/s.

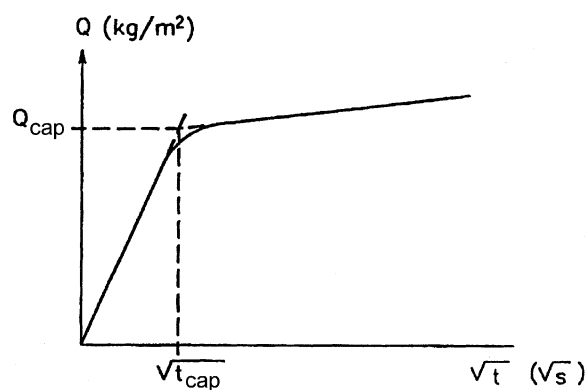


**Figure 11** The water absorption coefficient is the slope of the starting line (i.e., water absorption coefficient is  $Q_{cap} / \sqrt{t}_{cap}$ ).

the laboratory is 50%  $\pm$  5% RH, 23°C  $\pm$  1.5 °C during the tests. The bottom of the test specimen is 1 cm below the surface of the water.

### Measurements and Results

Measurements are performed according to prEN ISO 15148 (CEN 1998). At certain time intervals, the tube containing the test specimen is removed and weighed, after excess water is wiped off by a wet cloth. In the case of perlite and the coherent materials, water is allowed to drip off for 10 minutes while the tube is mounted on a 45° stand before the remaining water is wiped off by a wet cloth. The test is stopped when the weight has become constant. Then the absorbed water is

**TABLE 4**  
**Test Results for Capillary Water Uptake**

Material	Water absorption capacity [kg/(m <sup>2</sup> absorbing surface)]	Water absorption coefficient [kg/(m <sup>2</sup> $\sqrt{s}$ )]	Mean water content [weight% (105°C)]
Cellulose-1*	39	0.56	550
Cellulose-1**	67	0.81	657
Cellulose-3	37	0.27	453
Sheep's wool	2.5	0.012	79
Flax	2.9	0.016	387
Perlite	66	0.27	314
Perlite SR	0.5	0.005	3.4
Rock fiber	0.1	0.001	5.8
Glass fiber	3.0	0.03	394

\* 40 kg/m<sup>3</sup>  
 \*\* 65 kg/m<sup>3</sup>

measured as kg per square meter of immersed surface. The mean water content is calculated after drying the test specimen at 105°C until equilibrium. The difference between the mass at each weighing and the starting mass per unit area is calculated and plotted against the square root of the weighing times. From the resulting graph, the slope is the water absorption coefficient (see Figure 11). Table 4 shows the test results for capillary water uptake.

From the results, it can be concluded that perlite SR, sheep's wool, flax, rock fiber, and glass fiber have a small water absorption capacity and a small water absorption coefficient. Perlite and the three cellulose materials all have a high water absorption capacity. The influence of salt washout on the rate of liquid transfer is not tested. Furthermore, the physical structure is altered by the water absorption. Figure 12 shows the appearance of cellulose-1 ( $65 \text{ kg/m}^3$ ) after drying at  $105^\circ\text{C}$ . The test specimen is divided into four layers, which are dried and weighed individually for determination of the water content in each layer. The bottom side of the lower layer (shown at the top in Figure 12) has been 1 cm below the surface of the water. The layer 4 to 9 cm above the surface of the water (shown in Picture 2 in Figure 12) has a water uptake of  $390 \text{ kg/m}^3$ —about half of the value in the lowest 5 cm of the test specimen (Picture 1). This is similar to results given by Marchand and Kumaran (1994). Therefore, capillary water uptake in cellulose materials must be avoided.

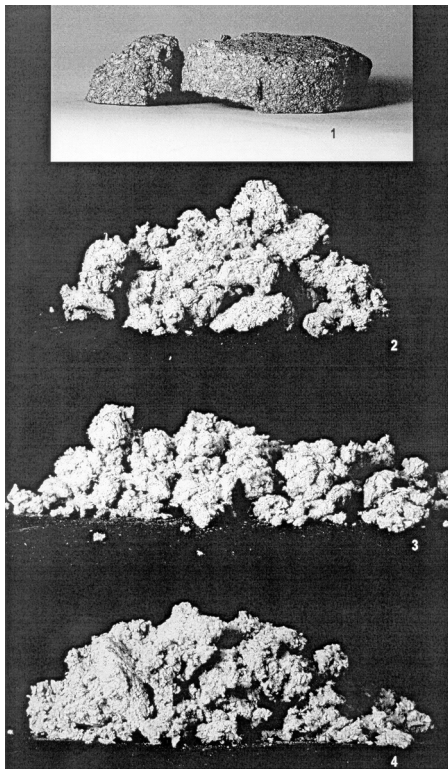


**Figure 12** Cellulose-1 ( $65 \text{ kg/m}^3$ ) after drying at  $105^\circ\text{C}$ . Picture 1 shows the lowest 5 cm of the test specimen (from 1 cm below the surface of the water to 4 cm above), Picture 2 shows the layer 4 to 9 cm above the surface of the water, Pictures 3 and 4 show the layers 9 to 14 cm and 14 to 19 cm above the surface of the water.

## MOISTURE BUFFER CAPACITY

Porous, absorbing materials emit water vapor to the air when RH decreases as the material reacts against the process—usually ventilation—that causes the decrease in RH. Water vapor is absorbed in the material again when RH rises. In this paper, this process is defined as moisture buffering. There is no international unit describing the moisture buffer capacity of a material, nor any international standard for measuring this capacity. This matter is debated in Padfield (1999). The experiment reported here is, therefore, a demonstration of how moisture moves into a wall insulated with absorbent organic fiber—in this case, sheep's wool—under isothermal conditions.

The experimental wall was constructed from gypsum board at the interior surface, then a vapor retarding spun-bonded polyolefin layer covering 200 mm of sheep's wool (Figure 13). The back of the wool was sealed by an aluminium

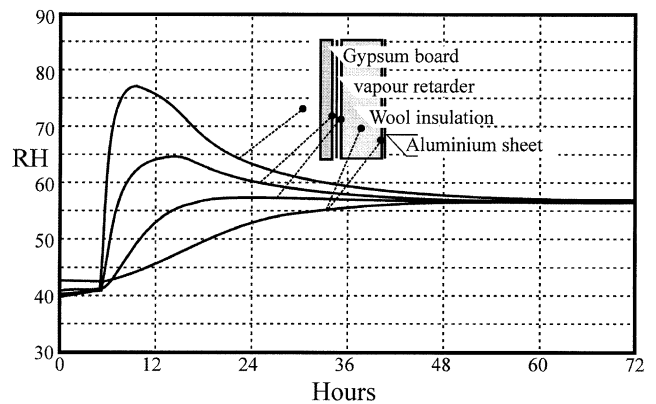


**Figure 13** Development of the relative humidity [%] through a wall after a sudden addition of water vapor to a room, here imitated by a stainless steel, airtight chamber. The wall consists of a gypsum plaster-board, a vapor retarder, and sheep's wool insulation. The backside is a sheet of aluminium. The test wall is preconditioned to about 42% RH. At hour five, the test chamber is supplied with a quantity of water vapor, which would cause condensation of  $20 \text{ g/m}^3$  water if the chamber were empty. The test wall absorbs the water vapor so effectively that the RH never exceeds 80%. At first, the plaster-board absorbs the water vapor after which it slowly diffuses through to the wool insulation behind. After 60 hours, the greater part of the water is stored in the wool, and the RH in the room has fallen to 57%. The wool insulation is, therefore, an effective moisture buffer in this closed chamber; but, in a real room, natural ventilation would have renewed the air several times before the wool had really started to absorb the water.

plate. This assembly was put in an airtight chamber, which contains a device that can emit or absorb water vapor in a measured amount. The RH in the chamber air is controlled by the interaction between the absorbing test wall in the chamber and the chamber air. By analyzing the test results, it can be concluded that absorbing sheep's wool behind a vapor retarder and a plaster board has no practical influence on the indoor climate of a house if the house is ventilated as recommended (i.e., 0.5 times per hour).

## DISCUSSION

The thermal conductivities of the materials are not much affected by RH until the dew point is reached at the cold side of the test specimen. In practice, condensation within the organic fibers will be catastrophic for cellulose fiber insulation, which is by far the most used of the organic insulators. The more coherent products—sheep's wool and flax—can resist short periods of condensation, but the evidence for migration of protective salts at high RH suggests that the owner of the building has more important things to worry about than increased heat loss. In situations where organic insulation can be used safely, the evidence is that the thermal insulation is hardly affected by relative humidity and may be almost as thermally effective as mineral fiber insulation in practical applications.

The results from the sorption measurements confirm previously published data for the pure materials but show that the salts added to improve fire and rot resistance increase the water absorption at a high RH. This will cause physical collapse of cellulose fiber and risk washing out the protective salts from sheep's wool and flax insulation. On Figure 7c, the desorption isotherm for flax insulation is always below the absorption isotherm due to washing out the protective salts. So much water is absorbed at high RH that the subsequent drying will be slower than with the pure fiber. One must conclude that these materials must never reach an RH above about 85%.

The water vapor permeability of these materials, measured at a steady state, is similar to that of mineral fiber insulation. In practical situations, a transient state can be dealt with by using the vapor water permeability measured by the steady-state method and by considering the material's moisture capacity. An experiment with sheep's wool insulation subjected to a sudden flux of water vapor demonstrates how water is absorbed into the fibers, moderating the climate within the structure.

Capillary water uptake is measured on organic materials that cannot keep their form during the test. The specimen height for both loose-fill materials and coherent materials decreases during the test. In this way, the density increases during the test. In other words, the results for capillary water

uptake are influenced by this increase in density, and the results may be used in this light.

## CONCLUSION

The thermal conductivities of the materials are not much affected by RH until the dew point is reached at the cold side of the test specimen. In practice, condensation within the organic fibers will be catastrophic for cellulose fiber insulation, which is by far the most used of the organic insulators. The more coherent organic fibers—sheep's wool and flax—can resist short periods of condensation.

The results from the sorption measurements confirm previously published data for the pure materials but show that the salts added to improve fire and rot resistance increase the water absorption at a high RH. This will cause physical collapse of cellulose fiber and risk washing out the protective salts from sheep's wool and flax insulation. So much water is absorbed at a high RH that the subsequent drying will be slower than with the pure fiber. One must conclude that these materials must never reach an RH above about 85%.

The water vapor permeability of these materials, measured at a steady state, is similar to that of mineral fiber insulation.

## REFERENCES

- CEN. 1998. prEN ISO 12572. *Hygrothermal performance of building materials—Determination of water vapour transmission properties*. CEN/TC89/WG10 N230. European Committee for Standardization.
- CEN. 1998. prEN ISO 15148. *Hygrothermal performance of building materials—Determination of water absorption coefficient by partial immersion*. CEN/TC89/WG10 N196. European Committee for Standardization.
- CEN. 1998. prEN ISO 12571. *Hygrothermal performance of building materials—Determination of hygroscopic sorption properties*. CEN/TC89/WG10. European Committee for Standardization.
- Hansen, K.K. 1989. Equipment for and results of water vapour transmission tests using cup methods. *Proceedings ICHMT Symposium—Heat and Mass Transfer in Building Materials and Structures*. Dubrovnik, Yugoslavia.
- Hansen, K.K., and H.B. Lund. 1990. Cup method for determination of water vapour transmission properties of building materials. Sources of uncertainty in the method. *Proceedings of the 2<sup>nd</sup> Symposium on Building Physics in the Nordic Countries*. Trondheim: Norwegian University of Science and Technology.
- Hansen, K.K. et al. 1999. Main Report. *Experimental investigation of the hygrothermal performance of different insulation materials* (in Danish). Denmark: Department of Structural Engineering and Materials and Department of Buildings and Energy, Technical University of Denmark. [http://www.by-og-byg.dk/forskning/alternativ\\_isolering/bkm-ibe.htm](http://www.by-og-byg.dk/forskning/alternativ_isolering/bkm-ibe.htm).

- Lackey, J.C., R.G. Marchand, and M.K. Kumaran. 1997. A logical extension of the ASTM Standard E96 to determine the dependence of water vapour transmission on relative humidity. *Insulation materials: Testing and Applications: Third Volume, ASTM STP 1320*, R.S. Graves and R.R. Zarr, eds. American Society for Testing and Materials.
- Lund Madsen, T. 1969. Modified guarded hot plate apparatus for measuring thermal conductivity of moist materials. *Supplément au Bulletin de l'Institut International du Froid. Commissions II & VI*. Liège: Institut International du Froid.
- Marchand, R.G., and M.K. Kumaran. 1994. Moisture diffusivity of cellulose insulation. *Journal of Thermal Insulation and Building Envelopes*, 4.
- Padfield, T. 1999. Humidity buffering of the indoor climate by absorbent walls. *Proceedings of the 5th Symposium on Building Physics in the Nordic Countries*. Göteborg: Chalmers University of Technology.
- Padfield, T., and D. Erhardt. 1987. The spontaneous transfer to glass of an image of Joan of Arc. Preprints of the Sydney Conference of the International Council of Museums (ICOM), Conservation Committee.
- Tye, R., and S.C. Spinney. 1979. A study of the effects of moisture vapour on the thermal transmittance characteristics of cellulose fibre thermal insulation. *Journal of Thermal Insulation*, Vol. 2 (April 1979): 175-196.